

$(p, \alpha)$  Reactions Induced by Protons in the Energy Range of 9.5–23 Mev

CLYDE B. FULMER AND CHARLES D. GOODMAN  
Oak Ridge National Laboratory,\* Oak Ridge, Tennessee

(Received June 5, 1959; revised manuscript received November 16, 1959)

An earlier study of  $(p, \alpha)$  reactions induced by 23-Mev protons has been extended by observing the outgoing alpha particles from nuclear reactions induced by protons of various energies between 9.5 and 23 Mev in numerous elements throughout the periodic table. Alpha-energy distributions and absolute differential  $(p, \alpha)$  cross sections were measured at 90 deg. From the integrals of the alpha-energy distributions, excitation functions for  $(p, \alpha)$  reactions were determined. Excitation functions for  $(p, \alpha)$  reactions in targets for which compound nuclei are integral numbers of alpha particles are qualitatively different from those of other targets. Alpha-energy distributions for targets with  $Z \lesssim 50$  (except for F and Al) are peaked at about the same energy for incident proton energies of 9.5–23 Mev; this may be interpreted as evidence that the Coulomb barrier is lowered for alpha-particle emission from excited compound nuclei.

## INTRODUCTION

IN a previous paper<sup>1</sup> a survey of  $(p, \alpha)$  reactions induced by 23-Mev protons in targets of a wide range of atomic number was presented. Alpha-particle energy distributions and absolute differential cross sections were measured at 30, 60, 90, 120, and 150 deg. The survey showed that alpha particles from heavy elements and from the high-energy parts of the spectra from light elements are produced by direct interaction reactions; for targets of  $Z \lesssim 50$ , a large fraction of  $(p, \alpha)$  reactions proceeds by compound nucleus reactions. The most important result of the survey, however, is evidence that alpha particles experience a lower Coulomb barrier in leaving an excited compound nucleus than in entering a ground-state nucleus.

This earlier survey of  $(p, \alpha)$  reactions has been extended by observing the outgoing alpha particles from reactions induced by protons of various energies between 9.5 and 23 Mev in numerous elements throughout the periodic table. Alpha-energy distributions were determined for a range of proton energies, and from the integrals of the energy distributions the excitation functions for  $(p, \alpha)$  reactions were determined.

## EXPERIMENTAL

The energy analyzed external 23-Mev proton beam of the Oak Ridge National Laboratory 86-Inch Cyclotron was used for these experiments. Lower proton energies were achieved by use of absorbers; part of the experimental arrangement is shown schematically in Fig. 1. The incident proton beam is defined by collimator A, passes through an aluminum absorber on the absorber wheel, is redefined by collimator B, passes through a target foil on the target wheel, and is collected in a Faraday cup which monitors the beam. Collimator C defines a beam of outgoing particles that enters the detector. All data were obtained with the detector at 90 deg from the proton beam. Since the absorber is a

strong source of gamma rays, a lead shield is used between the absorber and the detector; additional lead shielding, not shown in Fig. 1, was used to reduce the intensity of gamma rays, from collimator A and the Faraday cup, at the detector.

A blank target space was left on the target wheel during most data runs. The shielding of the detector from the beam collimators and absorbers was tested by rotating the blank space on the target wheel into the beam. No detector counts were observed when this test was made. The beam monitoring system was tested by varying the target-to-Faraday-cup distance and repeating data runs. The data were reproducible within counting statistics, and independent of the target-to-Faraday-cup distance, for a range of distances. These tests demonstrated the adequacy of the experimental arrangement in the scattering chamber.

The  $(p, \alpha)$  reactions were studied by observing the outgoing particles which passed through a port in the

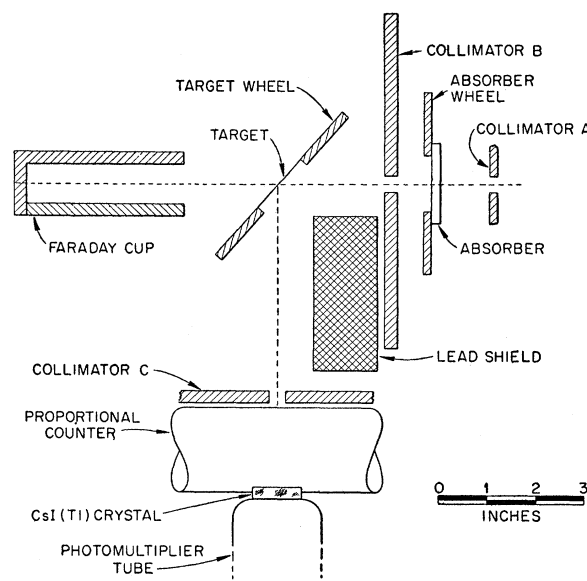


FIG. 1. Experimental arrangement in the scattering chamber for studying  $(p, \alpha)$  reactions with protons of various energies.

\* Operated for the U. S. Atomic Energy Commission by Union Carbide Corporation.

<sup>1</sup> C. B. Fulmer and B. L. Cohen, Phys. Rev. **112**, 1672 (1958).

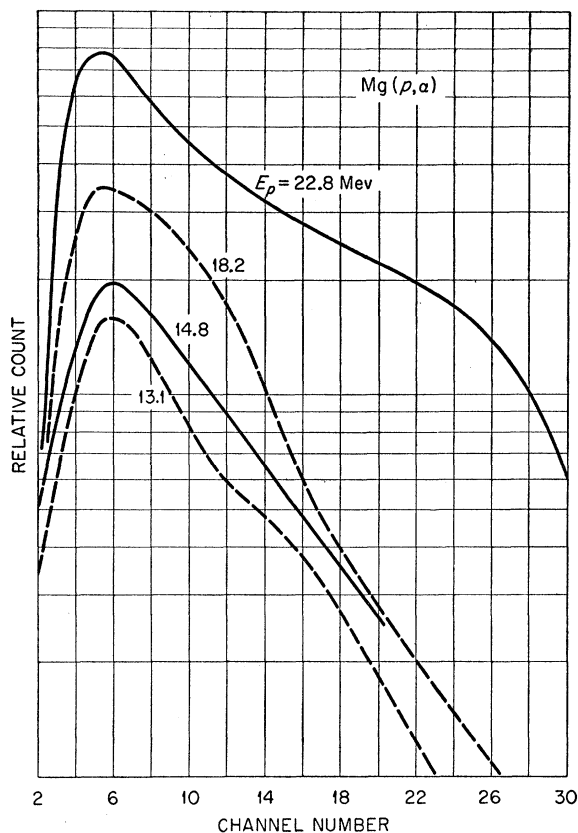


FIG. 2. Energy spectra of alpha particles from  $(p,\alpha)$  reactions induced in Mg by protons of various energies. These spectra were observed at 90 deg from the proton beam.

wall of the 11-in. diam. scattering chamber, located 90 deg from the proton-beam direction. As in the earlier experiments,<sup>1</sup> the particles were detected by a proportional counter-scintillation counter telescope. Alpha-particle energy distributions were determined by pulse-height analysis of the scintillation-counter pulses; a coincidence gate on the 20-channel pulse-height analyzer was triggered with proportional-counter pulses which passed an integral discriminator; thus background pulses were eliminated from the data. Additional details of the particle detector and of the energy calibration are given in reference 1.

For part of the data, the proportional counter-scintillation counter telescope was used with a particle-identification system.<sup>2</sup> This system provides for a means of selecting gate pulses so that the entire spectrum can be observed at one setting. Thus the amount of cyclotron time required for obtaining the data is reduced. A check on the  $(p,\alpha)$  cross sections integrated over energy was provided by counting alpha-particle gate pulses.

The procedure used for making a data run is as follows: A target wheel and absorber wheel are installed

in the scattering chamber. The aluminum absorbers are of various thicknesses that reduce 23-Mev protons to energies down to 9.5 Mev. Both wheels may be rotated by remote control so that targets and absorbers are changed without interrupting the cyclotron operation. The proportional counter is filled to a pressure of 12 cm Hg with a 90% A-10% CH<sub>4</sub> gas mixture. A pulse-height spectrum of the proportional counter or particle identification system output is then measured, and the proper setting for the gate-pulse discriminator is determined. The gain of the scintillation counter is set by adjusting the photomultiplier voltage until the elastically scattered protons are counted in the proper channel. The energy calibration of the crystal is described in reference 1; in general, the absolute energy calibration is accurate to within  $\frac{1}{2}$  Mev at all energies. After the preliminary arrangements and measurements are finished, the  $(p,\alpha)$  energy spectra are obtained. From the integral of the alpha-particle energy spectra, absolute cross sections are determined; no resolution of single levels of the residual nuclei was made in this work.

## RESULTS

Energy distributions of alpha particles observed from protons of various energies on targets of Mg, Ni, and Rh are shown in Figs. 2, 3, and 4, respectively. The data were obtained with counting statistics that allow standard deviations of 10% or less for the central portion of each curve. Similar results were obtained for

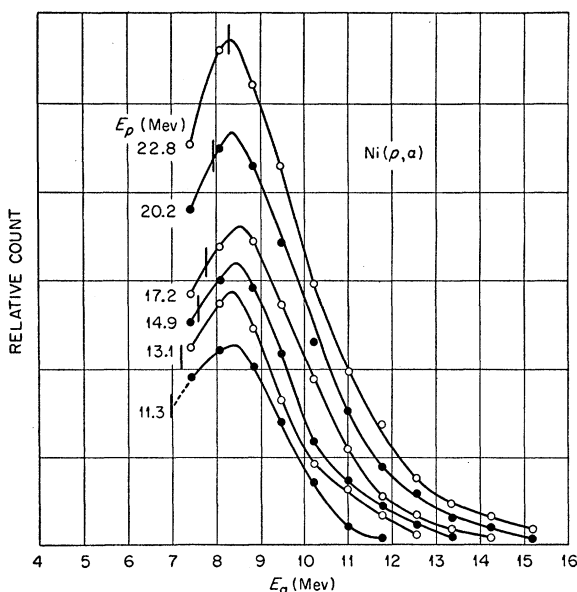


FIG. 3. Energy spectra of alpha particles from  $(p,\alpha)$  reactions induced in Ni by protons of various energies.  $E_\alpha$  is the total kinetic energy of the emitted particle and residual nucleus in the center-of-mass system. These spectra were observed at 90 deg from the proton beam. The vertical cuts on the curves show how the energy distribution peaks would vary with  $E_p$  if the Coulomb barrier were constant with excitation energy of the compound nucleus (see text).

<sup>2</sup> C. D. Goodman and J. B. Ball, submitted to Phys. Rev.

all other targets with  $Z \leq 50$  except for fluorine and aluminum. Because of the very low Coulomb barrier of fluorine, the alpha-energy spectra extend below 5 Mev where the energy calibration of the scintillation detector is very nonlinear. Hence, the  $(p, \alpha)$  data for that element were used to determine an excitation function only. In the case of aluminum, the alpha-energy spectra, for incident proton energy less than  $\sim 18$  Mev, have more than one maximum. The energy spectra of alpha particles observed from other targets exhibit the characteristic features of the data shown in Figs. 2, 3, and 4; the peaks occur at energies that increase slowly with atomic number of the target, and for each target they occur at approximately the same alpha-particle energy for the proton energy range of 9.5–23 Mev.

Excitation functions for  $(p, \alpha)$  reactions are shown in Fig. 5, and a tabulation of targets,  $Q$  values, and differential  $(p, \alpha)$  cross sections for 23-Mev protons is given in Table I. These data represent the average of two or more complete runs for each target. The scintillation-counter data were checked against data obtained from pulse-height analysis of the particle-identification system output. This check verified that the gating pulses represented the total alpha spectrum uncon-

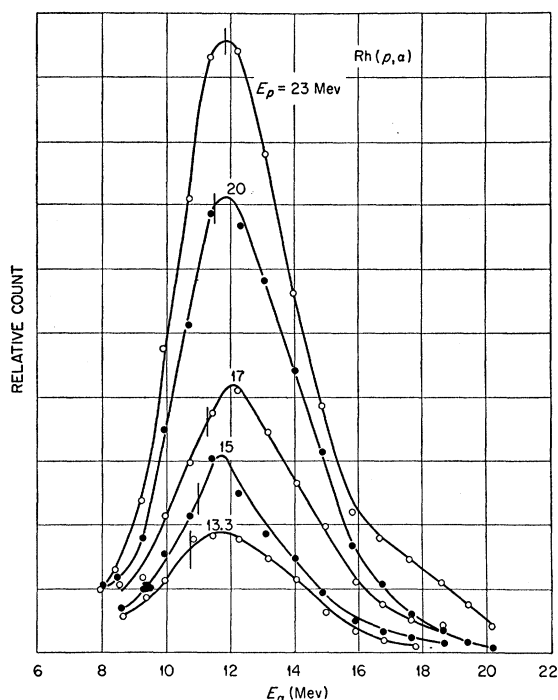


FIG. 4. Energy spectra of alpha particles from  $(p, \alpha)$  reactions induced in Rh by protons of various energies.  $E_\alpha$  is the total kinetic energy of the emitted particle and residual nucleus in the center-of-mass system. These spectra were observed at 90 deg from the proton beam. The vertical cuts on the curves show how the energy distribution peaks would vary with  $E_p$  if the Coulomb barrier were constant with excitation energy of the compound nucleus (see text).

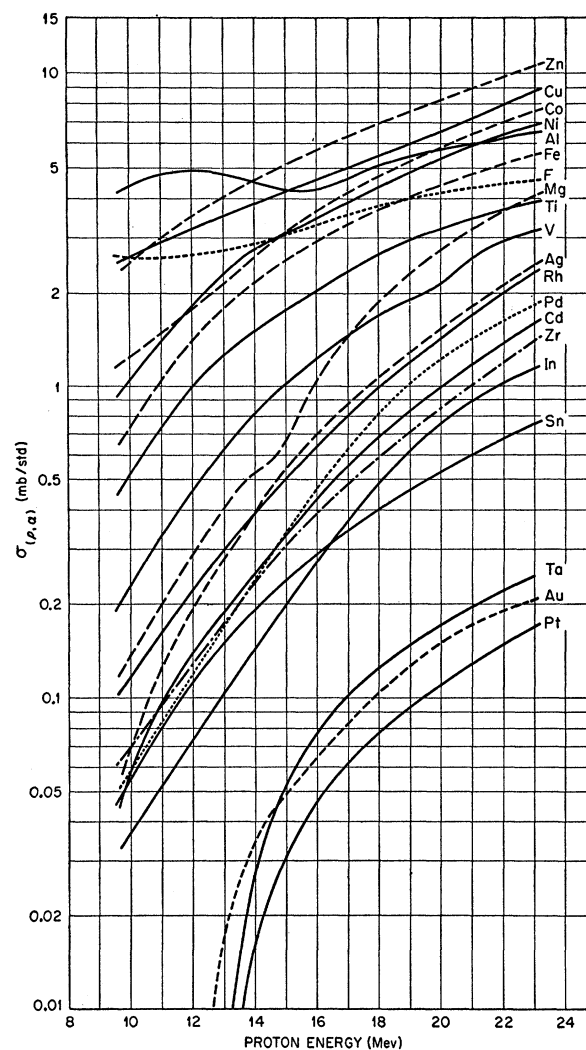


FIG. 5.  $(p, \alpha)$  excitation functions for various targets. The cross sections were computed from the integrals of the alpha-energy distributions observed at 90 deg. The curves were determined from data obtained at proton energy intervals  $\leq 3$  Mev.

taminated by pulses from other particles. The probable errors are less than 5% except for Ta, Pt, and Au; for these targets the probable errors at the lowest proton energies are as large as 15%.

Total  $(p, \alpha)$  cross sections may be obtained by multiplying the differential cross sections shown in Fig. 5 by the factor  $4\pi$ ; for the heavy targets (Ta, Pt, and Au), this product should be increased by a factor of 2 because of the strong forward peaking<sup>1</sup> of the angular distributions of alpha particles emitted from these targets.

In Fig. 5 the excitation function for  $(p, \alpha)$  reactions in F and Al are qualitatively different from those of other targets in that they do not decrease appreciably for lower proton energies. The  $(p, \alpha)$  reaction in the stable isotopes of F and Al leave residual nuclei that

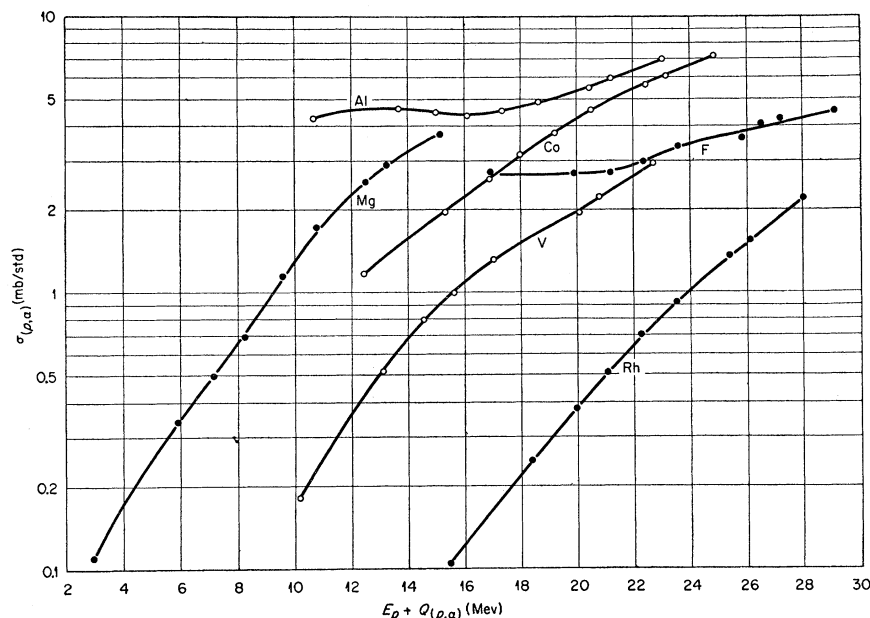


FIG. 6. Cross sections for  $(p, \alpha)$  reactions in various targets plotted as functions of energy available for alpha-particle emission. These data were obtained with the detector 90 deg from the proton beam. For F and Al the compound nuclei are integral numbers of alpha particles.

are even-even and which have low level densities; however, even-even residual nuclei may also result from  $(p, \alpha)$  reactions in the principal isotopes of V, Co, and Rh. The flat shape of the excitation function observed for F, Al, is not observed for V, Co, and Rh.

One feature of  $(p, \alpha)$  reactions in F and Al that is unique among the targets in Fig. 5 is that the compound nucleus (and hence the residual nucleus) consists of an integral number of alpha particles. In Fig. 6 cross sections for  $(p, \alpha)$  reactions in F, Al, Mg, V, Co, and Rh are plotted as functions of maximum energy available

for alpha-particle emission. There also the curves for F and Al are qualitatively different from the others. This indicates that the effect is not simply due to  $Q$  value differences.

#### DISCUSSION

The data presented earlier<sup>1</sup> for targets with  $Z \lesssim 50$  indicate, by the energy and the angular distributions of the alpha particles, that for these targets a large fraction of the alpha particles from  $(p, \alpha)$  reactions results from compound nucleus reactions. The data are most readily explained in detail, however, by assuming that an alpha particle encounters a lower Coulomb barrier in leaving an excited compound nucleus than in entering a ground-state nucleus. Evidence for the lower Coulomb barrier is also exhibited by the data of Fig. 5 and Table I. In particular, the ratio of  $\sigma(p, n)/\sigma(p, \alpha)$  and the sensitivity of  $\sigma(p, \alpha)$  to  $Q$  value and proton energy are very different from the values predicted if one assumes a Coulomb barrier for alpha-particle emission that corresponds to  $r_0 = 1.5$  fermis (1 fermi =  $10^{-13}$  cm) in the tables of Blatt and Weisskopf<sup>3</sup>; this is in good agreement with the barrier for ground-state nuclei as observed in numerous experiments in which ground-state nuclei are bombarded with charged particles. Numerical examples are discussed in reference 1, where it is shown that for  $(p, \alpha)$  reactions induced by 23-Mev protons, a Coulomb barrier corresponding to  $r_0 = 1.9$  fermis (extrapolated from the tables of Blatt and Weisskopf) gives much better agreement between experimental results and predictions of the statistical model of nuclear reactions.

TABLE I. Targets, atomic numbers,  $Q$  values, and differential  $(p, \alpha)$  cross sections measured at 90 deg for 23-Mev protons.<sup>a</sup>

Target	Z	$Q(p, \alpha)$ (Mev)	$Q(p, n)$ (Mev)	$\sigma(p, \alpha)$ for $E_p = 23$ Mev (mb/sterad)
F	9	8.1	-4.1	4.60
Mg	12	-6.0	-12.7	4.05
Al	13	1.7	-5.7	6.50
Ti	22	-2.6	-4.8	3.90
V	23	1.1	-1.5	3.10
Fe	26	-1.4	-5.5	5.50
Co	27	3.3	-2.0	7.40
Ni	28	-0.7	-9.5	7.00
Cu	29	3.7	-3.9	8.80
Zn	30	2.1	-6.5	11.0
Zr	40	-0.5	-3.6	1.40
Rh	45	6.2	-1.5	2.35
Pd	46	2.9	-3.3	1.85
Ag	47	6.2	-1.7	2.45
Cd	48	3.2	-2.5	1.68
In	49	6.1	-0.4	1.15
Sn	50	2.4	-4.0	0.750
Ta	73	4.8	-0.9	0.245
Pt	78	6.3	-1.9	0.165
Au	79	7.6	-7.9	0.205

<sup>a</sup> The  $Q$  values shown here are weighted averages of the values for the stable isotopes of each element.

<sup>3</sup> J. M. Blatt and V. F. Weisskopf, *Theoretical Nuclear Physics* (John Wiley and Sons, Inc., New York, 1952), p. 353.

Further experimental evidence of the lowered Coulomb barrier for alpha-particle emission from excited compound nuclei is demonstrated by the results of the studies reported here; the peaks of the energy distributions do not shift with incident proton energy in the range of 9.5–23 Mev. This is seen as follows:

Assume that the energy distribution of emitted particles,  $N(E_\alpha)$ , is given by the product of a density of final states and a barrier-penetration factor. Then<sup>4</sup>:

$$N(E_\alpha) = \text{const} E_\alpha \sigma_c(E_\alpha) \omega(E_p + Q - E_\alpha), \quad (1)$$

where  $E_p$  and  $E_\alpha$  are, respectively, the center-of-mass kinetic energies in the proton-target and alpha-particle-residual-nucleus systems. Evidently, at the maximum of the energy distribution

$$(d/dE_\alpha) \log N(E_\alpha) = 0, \quad (2)$$

or

$$\frac{1}{E_\alpha} + \frac{1}{\sigma_c} \frac{d\sigma_c}{dE_\alpha} + \frac{d\omega}{dE_\alpha} = 0. \quad (3)$$

If one assumes that  $\omega$  is the commonly used form<sup>5</sup>

$$\omega = \text{const} \exp 2[a(E_p + Q - F_\alpha)]^{\frac{1}{2}}, \quad (4)$$

then at the maximum

$$\frac{1}{E_\alpha} + \frac{1}{\sigma_c} \frac{d\sigma_c}{dE_\alpha} - \frac{a^{\frac{1}{2}}}{(E_p + Q - E_\alpha)^{\frac{1}{2}}} = 0. \quad (5)$$

Equation (5) can be put in dimensionless form by multiplying by the Coulomb-barrier height  $B$  and making the substitution  $Y = E_\alpha/B$ ; Eq. (5) then becomes

$$\frac{1}{Y} + \frac{1}{\sigma_c} \frac{d\sigma_c}{dY} - \frac{(aB)^{\frac{1}{2}}}{(Y_{\text{max}} - Y)^{\frac{1}{2}}} = 0. \quad (6)$$

The experimental data show that  $E_\alpha$  at the maximum does not change as  $E_p$  is changed. Thus, it is evident from Eq. (5) that as  $E_p$  is increased, the term  $(1/\sigma_c)d\sigma_c/dE_\alpha$  evaluated at the maximum of the energy distribution must decrease.

It can be seen from the tables of Blatt and Weisskopf that  $\sigma_c$  is strongly dependent on the quantity  $Y$  and only weakly dependent on  $r_0$  as a separate parameter. One may, therefore, regard a change in the quantity  $(1/\sigma_c)(d\sigma_c/dE_\alpha)$ , evaluated at a constant value of  $E_\alpha$ , as equivalent to a change in  $B$ . Since a given  $E_\alpha$  corresponds to a higher excitation of the residual nucleus as  $E_p$  is increased, this interpretation implies that the Coulomb-barrier height decreases as the excitation energy of the compound nucleus increases but does not necessarily imply a change in nuclear size. The data presented here can be equally well interpreted by assuming that the shape of the Coulomb-barrier

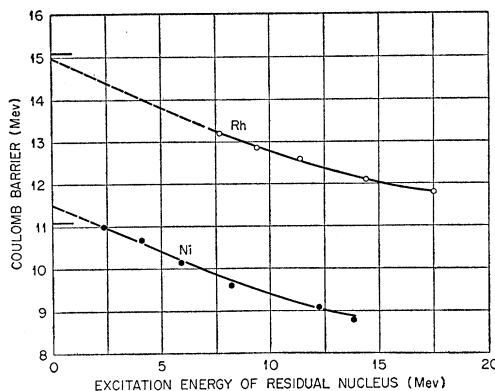


FIG. 7. Coulomb-barrier values calculated from Eq. (6) and plotted as a function of the excitation energy of the residual nucleus. The horizontal cuts on the ordinate axis correspond to the barrier values calculated for  $r_0=1.5$  fermis which agree with the experimental data obtained by bombarding nuclei in their ground states with charged particles.

penetration function changes with excitation energy so as to become less steep below the classical cutoff for a highly excited nucleus than for a nucleus in the ground state. In principle, a change in the shape of the barrier penetration function could be examined experimentally by comparing excitation functions for high-lying levels with those for low-lying levels.

For the residual nuclei from (*p*, $\alpha$ ) reactions in Ni and Rh (Figs. 3 and 4), the quantity  $(1/\sigma_c)d\sigma_c/dY$  was evaluated by using the tables of Blatt and Weisskopf. For each target, values of  $B$  were calculated that correspond to  $r_0=1.9$  fermis (as discussed in reference 1). Then values for  $a$  were determined by fitting Eq. (6) to the experimental data for 23-Mev proton energy. These values of  $a$  and  $B$  were then used to calculate the positions of the maximum of the alpha-energy distributions for lower proton energies. The positions of these calculated maxima are indicated by heavy vertical lines that cut the energy distribution curves in Figs. 3 and 4. It is very apparent that the peak shift required to satisfy Eq. (6) for constant values of  $B$  is not observed experimentally, and hence the data may be interpreted as evidence that the Coulomb barrier changes with excitation energy. Kikuchi<sup>6</sup> has suggested that a diffuseness of nuclear potential effectively lowers the Coulomb barrier. If surface diffuseness increases with nuclear excitation energy, the data presented here are consistent with this effect.

If, instead of inserting a constant value of  $B$  in Eq. (6), the experimentally determined value of the energy at which the alpha-energy distribution peak occurs is inserted, corresponding values of  $B$  may be found. This was done for the Ni and Rh data, and the results are plotted as functions of excitation energy of the residual nuclei (for alpha particles at the peaks of the energy distributions) in Fig. 7. The dotted portions of

<sup>4</sup> J. M. Blatt and V. F. Weisskopf, *Theoretical Nuclear Physics* (John Wiley and Sons, Inc., New York, 1952), p. 367.

<sup>5</sup> See reference 4, p. 371.

<sup>6</sup> K. Kikuchi, *Progr. Theoret. Phys.* **17**, 643 (1957).

the curves are extended to zero excitation energy to show extrapolated values of the Coulomb barriers for ground-state nuclei. The short, heavy horizontal lines on the figure show the barriers that correspond to  $r_0=1.5$  fermis and which are in agreement with the results of experiments in which charged particles bombard ground-state nuclei.

It should be pointed out that the above interpretation of the data is crucially dependent on the validity of the assumed form of the level density function. An alternate explanation of the lack of shift of the maxima in the alpha energy distributions with incident proton energy might be to take the level density to be of the form

$$\omega = \text{const} e^{(E_{\text{max}} - E)/T}, \quad (7)$$

where  $T$  is the nuclear temperature. Then no shift in the peak position would be expected with a change in  $E_{\text{max}}$ . Theoretical considerations<sup>7</sup> suggest that nuclear

<sup>7</sup> T. Ericson, Nuclear Phys. **6**, 62 (1958); T. Ericson, Nuclear Phys. **8**, 265 (1958).

temperatures are expected to vary only slowly with energy for low excitation energies. Alpha-particle inelastic-scattering data<sup>8</sup> have indicated nearly constant nuclear temperatures for excitation energies in the range of 4 to 10 Mev. A constant nuclear temperature interpretation of the  $(p,\alpha)$  data presented here, however, requires rather low values of temperature<sup>1</sup> for agreement between predicted and experimentally determined positions of energy distribution maxima.

#### ACKNOWLEDGMENTS

The authors wish to acknowledge the assistance of E. L. Olson for the maintenance of electronic equipment; M. B. Marshall, C. L. Viar, and F. A. DiCarlo in cyclotron operation; B. L. Cohen and J. B. Ball in various phases of the work; and the support and encouragement of R. S. Livingston.

<sup>8</sup> Fulbright, Lassen, and Poulsen, Kgl. Danske Videnskab. Selskab, Mat.-fys. Medd **31**, No. 10 (1959).